Semiconductor Physics, Quantum Electronics & Optoelectronics, 2008. V. 11, N 4. P. 311-318.

PACS 42.70.-a, 61.72.Ss, 61.80.Ed, 77.84.Fa

Microwave induced structural-impurity ordering of transition region in Ta_2O_5 stacks on Si

E.Yu. Kolyadina[1], R.V. Konakova[1], L.A. Matveeva[1], V.F. Mitin[1], V.V. Shynkarenko[1], E. Atanassova[2]
[1]*V. Lashkaryov Institute of Semiconductor Physics, NAS of Ukraine*
41 Nauky Prospect, 03028 Kyiv, Ukraine
Phone: +(380-44) 525-61-82; e-mail: konakova@isp.kiev.ua
[2]*Institute of Solid State Physics, Bulgarian Academy of Science*
72 Tzarigradsko Chaussée Blvd., 1784 Sofia, Bulgaria
Phone: +359-2-9795000 (448); e-mail: elenada@issp.bas.bg

Abstract. The effect of short-term microwave treatment (MT) on the electronic properties of interface in the Ta_2O_5–SiO_x–*p*-Si structures has been investigated. The samples of two types were studied: check ones (batch I) and those exposed to previous MT (batch II). The samples were aged (hold in air) at a temperature of ~300 K for two years. After that, they were exposed to MT during 2, 4, 6 and 8 s. Both before and after two-year aging and further MT, we measured, for all samples, the spectra of surface-barrier electroreflectance (SBER) and concentration depth profiles of the components in the structure, as well as the radii of curvature of heterosystem from which the intrinsic stress (IS) values were calculated. It was found that the transition energy E_g grows with time of MT for both type samples. This corresponds to decrease of compressing ISs in 27 % in the check sample (with more number of defect) and by 11 % in that previously exposed to MT. This fact indicates structural-impurity ordering of the Si–SiO_x interface. The surface quantum-dimensional effect occurred after MT. After two-year aging, energy quantization was observed in the previously irradiated sample for 6 s and in the check sample (with more number of defects) after MT for 8 s. The most probable mechanism of improvement of the near-surface properties of SiO_x–Si interface is discussed.

Keywords: microwave treatment, Ta_2O_5–*p*-Si heterostructure, interface, surface-barrier electroreflectance, intrinsic stresses, quantum-dimensional effect, structural-impurity ordering.

Manuscript received 25.09.08; accepted for publication 20.10.08; published online 30.10.08.

1. Introduction

In recent years, an interest in silicon metal–insulator–semiconductor (MIS) structures with a thin dielectric of high permittivity ε (high-*k* dielectrics) integrated in CMOS technologies has grown considerably. Using such structures, it is possible to realize high-density dynamic random-access memory (DRAM) [1-9] serving as basis for superpower computer systems. In this case, it is natural to require high uniformity and structural perfection of thin insulators and insulator–Si interfaces.

The surface quantum-dimensional effect at the insulator–semiconductor interface can serve as measure of semiconductor structural perfection. This effect is known to occur in MIS structures with high-quality insulator and perfect structure of insulator–semiconductor interface [10-12]. Ta_2O_5 ($\varepsilon = 25 \div 30$, gap energy $E_g = 4.45$ eV) belongs to such insulators. However, the formation of a Ta_2O_5 film on *p*-Si showed that the dielectric film has in fact two-layer structure: bulk Ta_2O_5 on ultrathin (~2 nm) SiO_x interface layer [13-15].

As we have shown earlier, MT of Ta_2O_5-Si stacks in MIS configuration changes their electrophysical parameters. In particular, they are improved due to structural-impurity ordering at the insulator–Si interface [16]. It turned out that (judging from the surface barrier electroreflectance (SBER) spectra obtained for the Ta_2O_5–Si test structures) a short-term MT leads to decrease of the collision broadening parameter Γ of the

SBER spectra, while the radius of curvature R of the test structure increases. This evidences relaxation of intrinsic stresses (ISs) in the Ta_2O_5 film. The time stability of the effects observed remained undetermined. This work makes up this deficiency.

2. Experimental samples and procedure

A. Sample preparation procedure

Tantalum pentoxide layers were deposited on *p*-Si(100) (resistivity of 15 Ω·cm) by rf reactive sputtering of a tantalum target in an Ar + O_2 mixture: oxygen content of 10%, working gas pressure of 3.3 Pa, rf power of 3.6 W/cm^2, deposition rate of 5 nm/min. The film thickness was 60 nm.

We studied the structures of two type samples: the check ones and those after previous MT with frequency of 2.45 GHz, radiating power of 1.5 W/cm^2 and time of 1+2.5 s. (The latter means that, after MT for 1 s, the sample was relaxing at room temperature for 1 min, and then was exposed to MT for 2.5 s; so the total time of MT was 3.5 s.) The microwave irradiation was made in the open space (in air) at room temperature.

Then both the untreated and those exposed to MT samples were relaxing at room temperature during two years. After this, the samples were exposed to MT for 2, 4, 6 and 8 s. Using a profilometer-profilograph, we measured radii of curvature of the bended systems studied. They served for calculation of IS in the insulator film, while the Si band structure parameters immediately under the insulator film were determined with SBER.

B. Measurement of radius of curvature and estimation of IS

The radii of curvature of the samples under investigation were measured (both before and after MT) with a profilometer-profilograph П-104 and calculated from the deflection l of the arc chord m (see profilogram in Fig. 1) using the following expression:

$$R = m^2 / 8l \,. \qquad (1)$$

The IS value, σ, in the film was calculated from the Stoney formula [see, e.g., 17]

$$\sigma = Ed^2 / 6(1-\nu)Rt \,, \qquad (2)$$

where d (t) is the substrate (film) thickness, ν is Poisson ratio (0.278 for Si), and E = 1.3×10^{11} Pa is Young's modulus for Si (100) [18].

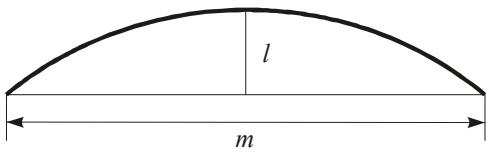

Fig. 1. Profilogram of a bended structure.

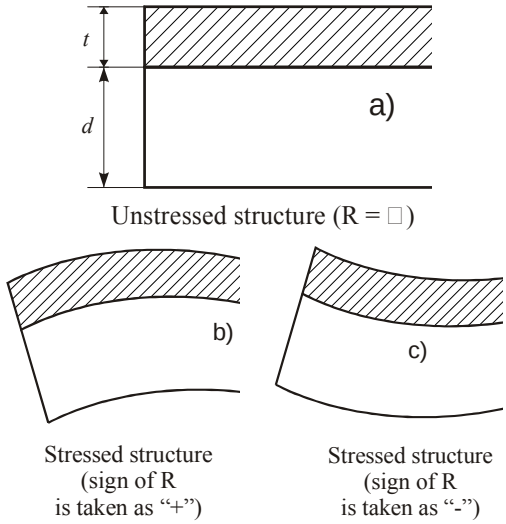

Fig. 2. Bending in two-layer Ta_2O_5–*p*-Si structures at different curvatures of the samples studied.

Shown in Fig. 2 is bending of a two-layer system for two different values of the radius of curvature on the film side. At $R = \infty$, the Ta_2O_5–Si is not stressed (Fig. 2a), at convex bending (Fig. 2b), the film is compressed, while the substrate is stretched. In this case, the sign of R is "+". At concave bending (Fig. 2c), the film is stretched, while the substrate is compressed, and the sign of R is "–".

C. Measurement of SBER spectra

We used the SBER technique [19] to determine how short-term MT and further holding of irradiated samples in air at room temperature during two years affect the degree of perfection of the near-surface silicon layers adjacent to Ta_2O_5. That technique registers small variations of the coefficient of reflection of monochromatic light from the sample surface due to modulation of surface potential with an electric field. An analysis of SBER spectra enables one to get information on the energy band structure of semiconductors, crystalline perfection of near-surface layers, quantum-dimensional effects and ISs. The collision broadening parameter Γ of SBER spectra serves as degree of perfection of the near-surface Si layer. This parameter characterizes scattering of optically excited charge carriers from imperfections of the surface under investigation. The parameter Γ decreases as the near-surface layer becomes more perfect, and increases as perfection of the near-surface Si layer is reduced.

The SBER spectra were taken using an automated facility based on a double monochromator ДМР-4. That facility ensured desired signal linearization in energy (with spectral resolution of 3 meV) and automatic division of a variable signal (modulated with an electric field) by a constant signal of light reflection (with sensitivity of 10^{-5}). The SBER spectra were measured using the electrolytic method, in the 0.1 normal water solution of NaCl, at room temperature; the photon energy range was 3.2÷3.6 eV.

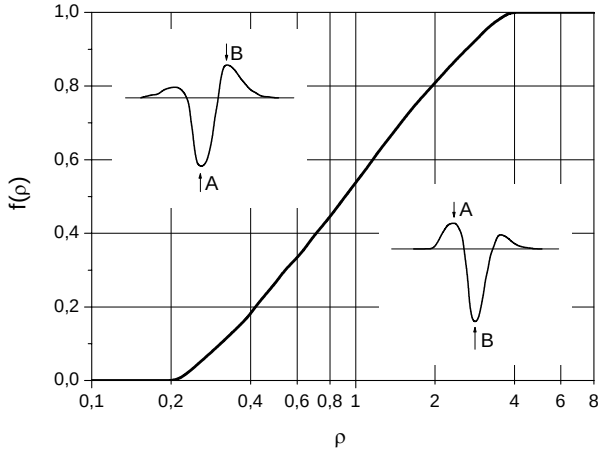

Fig. 3. Function $f(\rho)$ used for determination of the critical point energy E_g. A(B) - SBER spectrum of *n*-type (*p*-type) semiconductor.

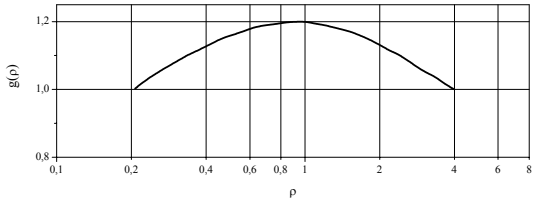

Fig. 4. Function $g(\rho)$ used for determination of the parameter Γ.

The transition energy E_g (the gap at the critical point of the Brillouin zone) was determined as

$$E_g = E_A + (E_B - E_A) \cdot f(\rho), \quad (3)$$

where E_A (E_B) is the energy position of the peak A (B) in the electroreflectance spectrum (see Fig. 3). Here $f(\rho)$ is function of the spectrum asymmetry parameter ρ

$$\rho = -(\Delta R / R)_B / (\Delta R / R)_A . \quad (4)$$

That function (calculated in [20]) is presented in Fig. 3.

The theory of low-field SBER spectra enables one also to determine the Lorentz (collision) broadening parameter Γ that characterizes the total energy scattering of optically excited charge carriers at the semiconductor surface (i.e., the surface quality). That parameter does not specify the scattering mechanisms but involves all the scattering processes occurring at the surface under consideration and leading to SBER spectrum broadening. To determine the collision broadening parameter Γ, the following expression is used:

$$\Gamma = (E_B - E_A) g(\rho) . \quad (5)$$

The function $g(\rho)$ (calculated in [21]) is presented in Fig. 4.

We estimated the gap E_g and parameter Γ (using the three-point technique) from energy position of the predominant peaks in the SBER spectrum according to [20, 21], considering the ratio of their intensities. Both the value and sign of IS in the substrate were determined from the difference ΔE_g of the transition energies in Si at the heterosystem interface (Tables 1 and 2) and the value $E_g = 3.38$ eV in the unstrained silicon sample [22], taking into account the coefficient $dE_g / d\sigma$. In silicon, contrary to germanium and gallium arsenide, the transition energy E_0' is decreased under compressing strains [23]. The corresponding coefficient is $dE_g / d\sigma = 1.5 \times 10^{-11}$ Pa ; the σ value can be estimated as

$$\sigma = \Delta E_g / (dE_g / d\sigma) . \quad (6)$$

D. Concentration depth profiles of heterostructure components

The concentration depth profiles of the Ta_2O_5–SiO_x-Si structure components were taken (both before and after MT) with a LAS-2000 device using the Auger electron spectroscopy, at layer-by-layer etching of the samples with 1 keV argon ions.

Table 1. Electronic parameters and stresses of substrate in non-irradiated (initial) Ta_2O_5–SiO_x–Si structure, t = 60 nm.

Time of MT, s	E_g, eV	ΔE_g, eV	Γ, meV	T, 10^{-15} s	σ, 10^9 Pa	$E_g + e_1$, eV	e_1, eV	L, nm
0	3.312	0.068	124	5	4.5	–	–	–
2	3.335	0.045	120	5.48	3	–	–	–
4	3.345	0.035	114	5.7	2.3	–	–	–
6	3.348	0.032	105	6.26	2.1	–	–	–
8	3.356	0.024	90	7.3	1.6	3.426	0.07	3.3

Table 2. Electronic parameters and stresses of substrate in irradiated Ta_2O_5–SiO_x–Si structure, t = 60 nm.

Time of MT, s	E_g, eV	ΔE_g, eV	Γ, meV	τ, 10^{-15} s	σ, 10^9 Pa	$E_g + e_1$, eV	e_1, eV	L, nm
0	3.340	0.040	96	6.85	2.6	–	–	–
2	3.342	0.038	95	6.92	2.5	–	–	–
4	3.345	0.032	94	7.0	2.1	–	–	–
6	3.373	0.007	85	7.7	0.47	3.513	0.140	2.14

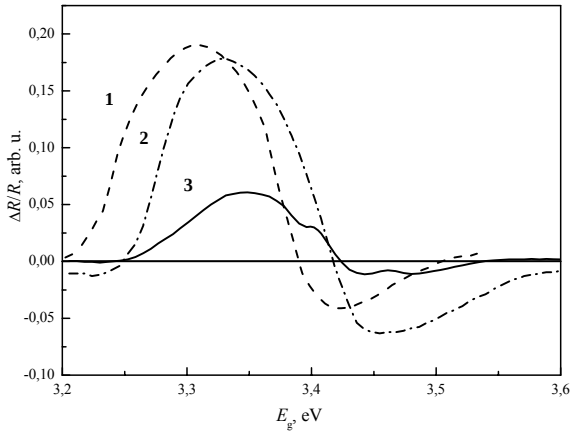

Fig. 5. SBER spectra of Ta_2O_5–Si structure (batch I, without pre-MT after two-year aging): 1 – before; 2 (3) – after 4 (8) s MT.

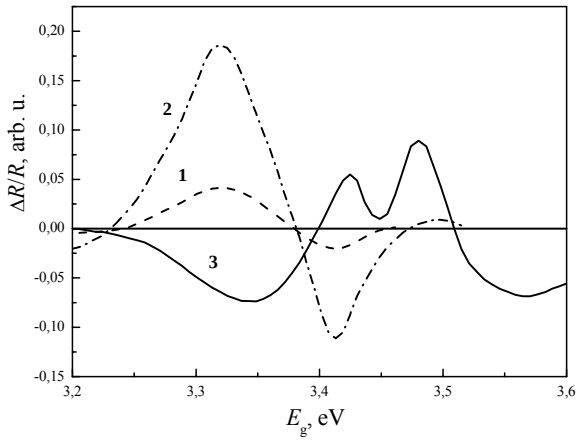

Fig. 6. SBER spectra of Ta_2O_5–Si structure (batch II, exposed to pre-MT and two-year aging): 1 – before; 2 (3) – after 4 (6) s irradiation.

3. Experimental results and discussion

Silicon is indirect-gap semiconductor with $E_g = 1.12$ eV. Indirect transitions cannot be registered with the SBER technique due to small oscillator strength for them. Therefore, we studied the transition whose energy is nearest to that of the indirect transition close to 3.4 eV (the E_0'-transition in the center of the Brillouin zone).

The SBER spectra for the samples from batch I taken at different times of further MT are shown in Fig. 5. Table 1 summarizes the data obtained from those spectra (transition energy E_g, broadening parameter Γ, IS σ and energy relaxation time τ for charge carriers). Figure 6 presents the SBER spectra for the samples from batch II (exposed to previous MT for 3.5 s and aged during two years) taken at different times of further MT. The parameters obtained from the spectra of those samples are given in Table 2.

The energy relaxation time for optically excited charge carriers is $\tau = \hbar/\Gamma$. Their mobility also is inversely proportional to the broadening parameter Γ.

One can see from the SBER spectra (Figs. 5 and 6) that, under certain conditions of microwave irradiation, the spectral peaks are split. We relate this splitting to quantization of charge carrier energy in a quantum well that appeared at the boundary on the substrate side after radiation ordering of the substrate structure owing to IS decrease.

The influence of the quantum-dimensional effects on the electronic properties of materials becomes pronounced, if the size of localization area for free charge carriers is comparable to their free path or to de Broglie wavelength. In this case, the motion of charge carriers is confined in that direction, and their energy spectrum is quantized. One should discriminate the bulk size effects (that exist, for example, in superlattices) and the surface size effects (that exist at the interfaces with a triangular quantum well). At the surface quantum-dimensional effect, the energy quantization occurs for charge carriers of one type only (either electrons or holes).

Along with the principal transition at the energy E_g, those involving the quantized levels at the energies $E = E_g + e_n$ (where e_n is the energy of a level in the well, $n = 1, 2, 3\ldots$) also appear in the SBER spectrum for a sample with a quantum well. The energy e_n is determined by the level number n, quantum well width L and the value of the interband effective mass m^* at the critical point of the Brillouin zone. For p-Si, $m^* = 0.119m_0$ (where m_0 is the free electron mass) at the point Γ of the Brillouin zone.

$$e_n = \frac{\hbar^2 \pi^2 n^2}{2m^* L_n^2}. \qquad (7)$$

In the case of the bulk quantization, the energy of a quantized level increases with its number n (at a constant quantum well width L) and decreases as L grows.

In our experiments, we observed the only level (after MT for 6 s for the samples from the batch II and for 8 s for those from the batch I). One can see from Tables 1 and 2 that the quantum well width decreases as the quantized level energy increases: $L = 3$ nm for $e_1 = 70$ meV and $L = 2.14$ nm for $e_1 = 140$ meV.

The data presented in Tables 1 and 2 show the transition energy increases with time of MT for the samples from both batches. This corresponds to reduction of compressing ISs in Si at the interface. For the samples from the batch I, E_g increases from 3.312 eV up to 3.356 eV after MT during 8 s, while changing from 3.340 eV to 3.373 eV after MT during 6 s for the samples from the batch II. In this case, Γ decreases from 124 meV down to 90 meV (by 27%) and from 96 meV down to 85 meV (by 11%), respectively. The ISs in the substrate decrease from 4.5×10^9 Pa down to 1.6×10^9 Pa (by 64%) (batch I) and from 2.6×10^9 Pa down to

4.7×10^8 Pa (by 82%) (batch II), while τ increases from 5×10^{-15} s up to 7.3×10^{-15} s (by 31%) (batch I) and from 6.85×10^{-15} s up to 7.7×10^{-15} s (by 12%) (batch II). These results mean that the process of radiation-enhanced IS relaxation and interface ordering are proceeding more intensely in a less perfect structure.

We measured the heterostructure bending radii to determine presence of IS in the film and variation of IS value as function of the samples previous history and MT duration. The results obtained showed the film always was on the concave size of the sample. This means that there existed stretching ISs. For the samples from the batch I, the heterostructure bending radii increased from 10 m up to 19.7 m (by 50%); after MT for 8 s, IS decreased by two times, from 5.98×10^9 Pa down to 3×10^9 Pa. For the samples from the batch II, the heterostructure bending radii increased from 17.3 m up to infinity (the structure became straight) after MT for 6 s, and ISs in the film dropped from 3.4×10^9 Pa down to zero. Therefore, the radiation-enhanced processes were proceeding in the film too. Their intensity is determined by previous technological history of the sample (pretreatment before aging).

A. Principal features of the effect of structural-impurity ordering

From the data presented in Tables 1 and 2, and in Figs 5 and 6, one can see that:

- ordering is observed under microwave irradiation at room temperature; no additional thermal annealing is required;
- the effect is characterized by well-pronounced localization in the near-interface region of the semiconductor. A direct proof to near-surface localization of the ordering effect was obtained when observing the quantum-dimensional effect and decrease of the parameter Γ at investigation of the SBER spectra (Fig. 5, 6). The region of MT-enhanced ordering ranges to a depth of several nanometers from the surface;
- we observed similar effect in the Al–Ta_2O_5–Si, (MIS) structure [16]. In this case, the improvement of *I–V* and *C–V* characteristics was also observed.
- the effect occurs in a limited range of irradiation doses.

Surface-enhanced radiation ordering in semiconductor structures has been studied mostly for the device structures based on III–V compounds (Schottky barrier, metal–insulator–semiconductor and insulator–semiconductor structures) exposed to rather low doses of ^{60}Co γ-radiation, high-energy (1÷4 MeV) electrons and some other types of radiation [24-26]. It was shown that transition of a metastable system to a more equilibrium (ordered) state might occur via one of the following processes, (or their combination, depending on the specific situation):

- radiation-induced gettering of the initial point defects at the interface (involving their annihilation) due to their interaction with the elastic stress field [27];
- radiation-ordered motion of impurities and intrinsic defects toward the surface, with forcing recombination-active impurities out of the sites into interstitials and vice versa (the Watkins effect) [28];
- radiation-ordered IS relaxation [29].

Judging from the above experimental data, one of such processes leading to MT-induced improvement of the parameters of SiO_x–Si interface is similar to the surface-enhanced ordering under action of rather low doses of γ-radiation that has been observed earlier [25, 26]. Indeed, interface is a region of two contacting materials that has a high density of defects. It can be considered as some transition layer (in our case, formed by SiO_x composition) that serves as inner drain for defects. One may follow the gettering action of the interface by comparing the component concentration profiles in the Ta_2O_5–SiO_x–Si contact (before and after MT) for one of the samples, (Fig. 7). As is seen the SiO_x–Si interface becomes more abrupt after MT, and the effective thickness of the interface transition layer decreases.

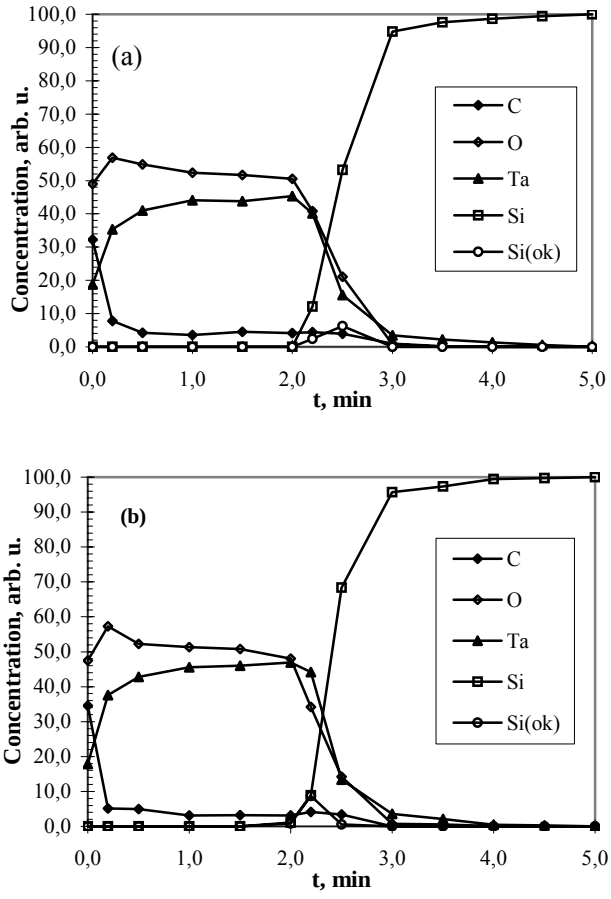

Fig. 7. Concentration depth profiles of Ta_2O_5–SiO_x–Si structure components: – before (a) and after 4 s MT of two-year aging at room temperature sample (b).

The SiO_x layer becomes narrower (by a factor of 2). As a result, the near-surface silicon layer is "cleaned" of oxygen, Ta_2O_5 is further oxidized, and the SiO_x–Si interface becomes more perfect. This leads to reduction of scattering of optically excited charge carriers on it. Therefore, the collision broadening parameter Γ decreases, while both the electron energy relaxation time τ and charge carrier mobility μ increase. Besides, after exposition to sufficient irradiation dose, the inversion of surface conductivity ($p \rightarrow n$) occurs in the Si substrate at the SiO_x–Si interface. This leads to polarity reversal for the SBER signal (fig. 6). It is known that electron mobility is usually higher than the hole one. Therefore, the collision broadening parameter (that is inversely proportional to charge carrier mobility) decreases, while the energy relaxation time of charge carriers ($\tau = \hbar/\Gamma$) increases. At concurrent decrease of the collision broadening parameter due to improvement of the interface, it became possible to observe surface quantization of electron energy in the triangle potential well that appeared because of surface conductivity inversion.

In this case, one should not exclude the dislocations that are produced in the course of MT-induced IS relaxation. They can serve as effective additional drain for point defects, thus increasing the gettering effect. The authors of [30] who investigated the effect of microwave radiation on defect structure of $Cd_{0.24}Hg_{0.76}Te$ crystals denoted the possibility of such process. A structural relaxation and reconstruction of structure defects ensemble in GaAs single crystals exposed to a short-term MT is observed in [31]. It should be noted that a transformation of dislocation structure of silicon after MT was also observed [32]. In this case, the MT-induced kinetics of residual strains relaxation differed considerably from the thermal one.

Primary localization of the effect near interface demonstrates its decisive role

- as defect drain;
- in formation (production) of centers promoting interaction between defects;
- in facilitation of the process of production (or annihilation) of MT-induced defects, since the bonds between atoms in the near-surface region are reduced as compared to bulk semiconductor.

B. Most likely mechanism of improvement of the SiO_x–Si interface near-surface properties

It was noted above that decrease of the parameter Γ is related to increase of charge carrier mobility μ in the near-surface Si layer adjacent to a thin SiO_x interface layer. The mechanism of μ increase under action of microwave radiation on a heterostructure is structural-impurity ordering in the near-surface Si layer and at the SiO_x–Si interface accompanied with IS relaxation (in this case, decrease of Γ correlates with growth of R for all structures studied) and radiation-enhanced mass transport of components in the SiO_x layer.

An important fact that confirms increase of μ in the near-surface Si layer is also polarity reversal of signal in the SBER spectrum for the sample 77 (curve 3 in Fig. 6) due to appearance of an inversion layer (it is known that charge carrier mobility in *n*-Si is considerably over that in *p*-Si). It was found that the width of the inversion layer adjacent to the SiO_x layer was ~ 3 nm. This indicates high quality of the heteroboundary in the sample 77 that formed in the course of microwave irradiation during 6 s after two-year relaxation and previous irradiation for 3.5 s.

The inversion layer is a potential well for electrons whose one wall is the SiO_x–Si interface, and the electrostatic potential forcing electrons against the boundary plays the role of another wall.

4. Conclusion

The data presented enable one to conclude that the observed improvement of parameters of the semiconductor interface region in the Ta_2O_5–SiO_x–Si system after a short-term MT, as well as after relaxation in the course of two-year aging followed with MT for 4–6 s, can be explained in terms of radiation defect-impurity gettering. It leads to ordering of the Si near-boundary region under MT for several seconds.

The processes of radiation ordering are proceeding more intensely in a thin layer that is adjacent to the SiO_x–Si interface. The effects of radiation ordering are pronounced more clearly in systems with less perfect interface.

The processes of MT-induced ordering in the Ta_2O_5–SiO_x–Si structures occur even at room temperature and are thermally stable. Therefore, possibility of their practical application for correction of parameters of the Ta_2O_5 stacks seems evident.

The Ta_2O_5/Si system exposed to previous MT remain stable after holding for two years at room temperature. Further, 2–6 MT s only improves the parameters of the SiO_x–Si interface.

References

1. The International Technology Roadmap for Semiconductors, Semiconductor Industry Association: *http://public.itrs.net* .
2. R.M. Wallace, G.D. Wilk. Alternative gate dielectrics for microelectronics // *MRS Bul*. **27**(3), p. 186-189 (2002).
3. E. Atanassova, T. Dimitrova. Thin Ta_2O_5 layers on Si as an alternative to SiO_2 for high-density DRAM applications, in: *Handbook of Surfaces and Interfaces of Materials*, Ed. H.S. Nalva, **4**, p. 439-479, San Diego, CA, Academic Press, USA, 2001.
4. J. Robertson, P.W. Peacock. Atomic structure, band offsets, growth and defects at high-*k* oxide:Si

interfaces // *Microel. Eng*. **72**(1-4), p. 112-120 (2004).
5. *High-k Gate Dielectrics.* Ed. M. Houssa. Inst. of Physics Publishing. Bristol, 2004.
6. E.P. Gusev, V. Narayanan, M.M. Frank. Advanced high-*k* dielectric stacks with poly Si and metal gates: Recent progress and current challenges // *IBM J. Res. Dev*. **50**(4/5), p. 387-410 (2006).
7. E. Atanassova, A. Paskaleva. Challenges of Ta_2O_5 as high-*k* dielectric for nanoscale DRAMs // *Microel. Reliab*. **47**(6), p. 913-923 (2007).
8. D. Spasov, E. Atanassova, D. Virovska. Electrical characteristics of Ta_2O_5 based capacitors with different gate electrodes // *Appl. Phys. A* **82**(1), p. 55-62 (2006).
9. V.A. Pilipenko, V.N. Ponomar, T.V. Petlitskaya. Charge properties of a capacitor system based on two-layer SiO_2–Ta_2O_5 insulator // *Inzh. Fiz. Zhurn*. **76**(1), p. 164-166 (2003) (in Russian).
10. Ya.Ya. Shik, L.G. Bakueva, S.F. Musikhin, S.A. Rykov. *Physics of Low-dimensional Systems*. Nauka, St-Peterburg, 2001 (in Russian).
11. E.F. Venger, L.A. Matveeva, P.L. Nelyuba. Effect of manufacturing technology on the parameters of interfaces in traditional and low-dimensional Si–SiO_2 structures // *Novi Tekhnologii. Naukovyi Visnyk KUEITU* **20**(2), p. 39-42 (2008) (in Russian).
12. E.F. Venger, L.A. Matveeva, P.L. Nelyuba, A.P. Klimenko. Diagnostics of low-dimensional systems with surface quantization of charge carriers energy, in: *Proc. VI Sc.-Tech. Conf. "Organization of Nondestructive Control of Production Quality in Industry"*, 18–25 April 2008, Taba, Turkey, p. 24-27 (in Russian).
13. N. Novkovski, E. Atanassova. Frequency dependence of the effective series capacitance of metal-Ta_2O_5/SiO_2–Si structures // *Semicond. Sci. Technol*. **22**(5), p. 533-536 (2007).
14. E. Atanassova, A. Paskaleva. Breakdown fields and conduction mechanisms in thin Ta_2O_5 layers on Si for high density DRAMs // *Microelectron. Reliab*. **42**(2), p. 157-173 (2002).
15. E. Atanassova, M. Kalitzova, G. Zollo, A. Paskaleva, A. Peeva, M. Georgieva, G.Vitali. High temperature induced crystallization in tantalum pentoxide layers and its influence on the electrical properties // *Thin Solid Films* **426**(1-2), p. 191-199 (2003).
16. E. Atanassova, N.S. Boltovets, E.Yu. Kolyadina, R.V. Konakova, J. Koprinarova, L.A. Matveeva, V.V. Milenin, V.F. Mitin, V.V. Shynkarenko, D.I. Voitsikhovskyi. Structural-phase ordering in Ta_2O_5–*p*-Si heterosystem enhanced by microwave processing, in: *Proc. 23rd Intern. Conf. on Microelectronics* (*MIEL 2002*) Niš, Yugoslavia, 12-15 May 2002, **2**, p. 531-534.
17. Hoffman R.W. Mehanical properties of thin condenced films. In: G. Hass, R.E. Thun, *Physics of thin films,* vol. 3. Academic Press, New York and London, 1966, p. 225-298.
18. A. Dargys, J. Kundratas. *Handbook on Physical Properties of Ge, Si, GaAs and InP.* Science and Encyclopedia Publishers, Vilnius, 1994.
19. P. Yu, M. Cardona, *Fundamentals of Semiconductors. Physics and Materials Properties*. Springer, Berlin, Heidelberg, 2002.
20. D.E. Aspnes, J.E. Rowe. High-resolution interband-energy measurements from electroreflectance spectra // *Phys. Rev. Lett*. **27**(4), p. 188-190 (1971).
21. D.E. Aspnes, J.E. Rowe. Asymptotic convolution integral for electric field effects on the interband dielectric function // *Solid State Commun*s **8**(14), p. 1145-1149 (1970).
22. R.Yu. Holiney, L.A. Matveeva, E.F. Venger. Investigation of the undersurface damages layers and silicon wafers // *SQO* **2**(4), p. 10-12 (1999).
23. G.L. Bir, G.E. Pikus. *Symmetry and Strain-Induced Effects in Semiconductors.* Wiley, New York, 1974.
24. O.Yu. Borkovskaya , N.L. Dmitruk , R.V. Konakova, V.G. Litovchenko, Yu.A. Tkhorik, B.I. Shakhovtsov. Effects of radiation-induced ordering in the layered structures based on III–V compounds // *Preprint No.6*, Inst. of Physics, AN UkrSSR, Kiev (1986) (in Russian).
25. N.L. Dmitruk. Surface-enhanced radiation ordering in semiconductor structures, in: *Fundamental Problems of Ion Implantation*, p. 60-81. Nauka KazSSR, Alma-Ata, 1987 (in Russian).
26. N.L. Dmitruk, R.V. Konakova. Surface-enhanced radiation ordering in semiconductor heterostructures // *Vestnik AN UkrSSR* No.6, p. 18-30 (1999) (in Russian).
27. *Physical Processes in Irradiated Semiconductors*, Ed. L.S. Smirnov. Nauka, Novosibirsk, 1977 (in Russian).
28. G.D. Watkins. A rewiev of EPR studies in irradiated silicon, in: *Effets des Rayonnement sur les Semi-conducteurs*, Ed. P. Baruch, p. 97-113, Dunod, Paris, 1964.
29. E.Yu. Brailovskii, L.A. Matveeva, G.N. Semenova, L.S. Khazan, Yu.A. Tkhorik. Radiation-stimulated relaxation of internal stress in heteroepitaxial systems // *Phys. status solidi* (*a*) **66**(1), p. K59-K62 (1981).
30. A.A. Belyaev, A.E. Belyaev, I.B. Ermolovich, S.M. Komirenko, R.V. Konakova, V.G. Lyapin, V.B. Milenin, E.A. Solov'ev, M.V. Shevelev. Influence of microwave treatment on the electrophysical characteristics of technically important semiconductors and surface-barrier structures // *Techn. Phys*. **43**(12), p. 1445-1449 (1998).
31. R.V. Konakova, P.M. Lytvyn, O.Ya. Olikh. Effect of microwave processing on deep levels in GaAs

and SiC single crystals // *Peterburgsky Zhurnal Elektroniki* No.1, p. 20-23 (2004) (in Russian).

32. V.I. Pashkov, V.A. Perevoshchikov, V.D. Skupov. Effect of annealing in a microwave radiation field on the residual strain and impurity composition of subsurface layers of silicon // *Techn. Phys. Lett*. **20**(4), p. 310-311 (1994).